



# HHS Public Access

Author manuscript

*Nat Struct Mol Biol.* Author manuscript; available in PMC 2015 November 01.

Published in final edited form as:

*Nat Struct Mol Biol.* 2015 May ; 22(5): 404–410. doi:10.1038/nsmb.3010.

## Translational control of the cytosolic stress response by mitochondrial ribosomal protein L18

Xingqian Zhang<sup>1</sup>, Xiangwei Gao<sup>1,4</sup>, Ryan Alex Coats<sup>1,2</sup>, Crystal S. Conn<sup>3</sup>, Botao Liu<sup>3</sup>, and Shu-Bing Qian<sup>1,2,3</sup>

<sup>1</sup> Division of Nutritional Sciences, Cornell University, Ithaca, NY 14853, USA

<sup>2</sup> Graduate Field of Nutritional Sciences, Cornell University, Ithaca, NY 14853, USA

<sup>3</sup> Graduate Field of Genetics, Genomics & Development, Cornell University, Ithaca, NY 14853, USA

### Abstract

In response to stress, cells attenuate global protein synthesis but permit efficient translation of mRNAs encoding heat shock proteins (HSPs). Despite decades since the first description of the heat shock response, how cells achieve translational control of HSP synthesis remains enigmatic. Here we report an unexpected role for mitochondrial ribosomal protein L18 (MRPL18) in the mammalian cytosolic stress response. MRPL18 bears a downstream CUG start codon and generates a cytosolic isoform in a stress-dependent manner. Cytosolic MRPL18 incorporates into the 80S ribosome and facilitates ribosome engagement on mRNAs selected for translation during stress. MRPL18 knockdown has minimal effects on mitochondria function, but substantially dampens cytosolic HSP expression at the level of translation. Our results uncover a hitherto uncharacterized stress adaptation mechanism in mammalian cells, which involves formation of a “hybrid” ribosome responsible for translational regulation during the cytosolic stress response.

### INTRODUCTION

Cell survival in a changing environment requires swift regulation of gene expression, including translational control of existing mRNAs<sup>1</sup>. Global translation is generally suppressed in response to most, if not all, types of cellular stress<sup>2,3</sup>. However, subsets of transcripts undergo selective translation to produce proteins that are vital for cell survival and stress recovery. One of the best-known examples is the heat shock protein 70 (Hsp70), whose synthesis is up-regulated in cells upon elevated temperatures or exposure to proteotoxic stress<sup>4,5</sup>. Despite the well-characterized transcriptional regulation<sup>6,7</sup>, it remains

Users may view, print, copy, and download text and data-mine the content in such documents, for the purposes of academic research, subject always to the full Conditions of use:[http://www.nature.com/authors/editorial\\_policies/license.html#terms](http://www.nature.com/authors/editorial_policies/license.html#terms)

Correspondence should be addressed to S.-B.Q. (sq38@cornell.edu).

<sup>4</sup>Present address: Institute of Environmental Medicine, Zhejiang University School of Medicine, Hangzhou, People's Republic of China.

#### AUTHOR CONTRIBUTIONS

X.Z. and S.-B.Q. conceived the original idea and designed the experiments. X.Z. performed the majority of the experiments, X.G. conducted luciferase reporter assays, R.A.C. assisted polysome gradient analysis, C.S.C. conducted [<sup>35</sup>S] metabolic labeling assays, B.L. assisted data interpretation, S.-B.Q. wrote the manuscript and all authors edited the manuscript.

elusive how efficient synthesis of HSPs persists when the translation machinery is generally compromised. It is commonly believed that the 5' untranslated region (5'UTR) of Hsp70 mRNA recruits the translational apparatus via a cap-independent manner<sup>8-11</sup>. However, neither the specific translation-promoting features of Hsp70 mRNAs nor the regulatory mechanism of the translation machinery have been clearly defined. In particular, it is unknown whether specialized ribosomes are required for efficient Hsp70 synthesis under stress conditions.

The ribosome is a large ribonucleoprotein complex composed of two subunits that associate upon the initiation of translation<sup>12</sup>. The small subunit decodes mRNA and the large subunit catalyzes peptide bond formation. In mammalian cells, there are two sets of ribosome particles residing in the cytoplasm and mitochondria respectively. Although ribosomal proteins (RPs) are all synthesized in the cytoplasm, they assemble into functional subunits in different subcellular compartments<sup>13</sup>. The mitochondrial RPs (MRPs) are encoded by nuclear genes, synthesized in the cytosol, imported into mitochondria for assembly, and responsible for translation of 13 mitochondrial mRNAs<sup>14</sup>. On the contrary, the cytosolic ribosomes are assembled within the nucleolus before export into the cytoplasm for mRNA translation. Because of their distinct composition and cellular localization, it is believed that there is little functional connection between mitochondrial and cytosolic ribosomes.

Here we set out to investigate whether specialized ribosomes are required in cytosolic stress response. We reported that the mitochondrial ribosomal protein L18 (MRPL18) bears a hidden CUG start codon downstream of the main initiation site. Stress conditions like heat shock trigger the CUG-initiated alternative translation, generating a cytosolic isoform of MRPL18. We found that the cytosolic MRPL18 integrates into the 80S ribosome complex in a stress-dependent manner and facilitates synthesis of stress proteins such as Hsp70. Our results uncover a hitherto uncharacterized stress adaptation mechanism in mammalian cells, which involves formation of a “hybrid” ribosome that promotes synthesis of stress proteins.

## RESULTS

### MRPL18 alternative translation produces a cytosolic isoform

We previously developed an approach called global translation initiation sequencing (GTI-seq) that allows precise mapping of alternative translation initiation sites (TIS) across the entire transcriptome<sup>15</sup>. The transcript encoding mitochondrial ribosomal protein L18 (MRPL18) bears several interesting features. First, MRPL18 shows three TIS sites with the annotated start codon (aTIS) flanked by an upstream TIS (uTIS) and a downstream TIS (dTIS) (**Fig. 1a**). While the uTIS codon is an AUG, the dTIS uses CUG as the initiator. Intriguingly, the CUG initiator is located immediately after the predicted mitochondrial targeting signal (MTS) of MRPL18 and within the same reading frame. It is likely that CUG-initiated translation produces a cytosolic isoform of MRPL18. However, the identical size of MRPL18(cyto) and the MTS-cleaved MRPL18(mito) renders them indistinguishable by standard immunoblotting.

To experimentally confirm the alternative translation of MRPL18, we constructed a series of MRPL18 mutants bearing myc-tags and examined their subcellular localization in HeLa

cells. The wild type MRPL18 was mostly localized in mitochondria as revealed by immunofluorescence staining (**Fig. 1b**). The vague cytoplasmic staining suggests that the CUG-initiated MRPL18(cyto) was not a major product under the normal growth condition. To show exclusively the CUG-initiated translation, we created a stop codon between the aTIS and the dTIS to prevent the synthesis of full length MRPL18. This mutant, MRPL18(C14A), exhibited a clear localization in the cytosol and the nucleus (**Fig. 1b**). The similar pattern was seen for MRPL18(ATG), a truncated version of MRPL18 lacking both the 5'UTR and the MTS. In contrast, MRPL18(G72A), a mutant with the dTIS mutated to CTA, showed a predominant mitochondrial localization. Together, these results indicate that MRPL18 bears a hidden downstream CUG start codon, whose initiation gives rise to a cytosolic isoform of MRPL18.

### MRPL18 undergoes stress-induced alternative translation

Notably, the CUG-only MRPL18(C14A) had much lower expression levels than other transgenes (**Fig. 1b** and **Supplementary Fig. 1a**), suggesting that the downstream CUG initiator is less efficient than the authentic AUG start codon. Interestingly, *MRPL18* is a heat shock-responsive gene<sup>16</sup>, and a recent study indicated that *MRPL18* is one of the direct targets of the heat shock transcription factor 1 (HSF1)<sup>17</sup>. Using a mouse fibroblast cell line lacking HSF1<sup>18</sup>, we confirmed the transcriptional up-regulation of *MRPL18* upon heat shock (**Supplementary Fig. 1b**). To investigate whether MRPL18 undergoes translational regulation in response to stress, we compared the abundance of transfected MRPL18 mutants in HeLa cells before and after heat shock. These transgenes maintained the similar mRNA levels in response to heat shock (**Supplementary Fig. 1c**), allowing direct evaluation of translational control. Immunoblotting showed two bands of transfected MRPL18, corresponding to the MRPL18 precursor and the MRPL18 species lacking the MTS (**Fig. 2a**, lane 3). The transfected MRPL18 undergoes less efficient processing than the endogenous counterpart presumably due to reduced mitochondrial import because the transgene lacks the 3'UTR of MRPL18<sup>19</sup>. As expected, the imported exogenous MRPL18 incorporates into mitochondrial ribosomes as evidenced by its co-sedimentation with other mito-ribosomal proteins (**Supplementary Fig. 1d**). Upon heat shock stress, the full length MRPL18(WT) showed a modest increase, whereas much less change was observed for MRPL18(ATG) that lacks both the 5'UTR and the MTS region (**Fig. 2a**, lanes 9 and 10). Remarkably, the CUG-only MRPL18(C14A) exhibited the strongest responsiveness despite its low basal levels in cells without stress (**Fig. 2a**, lanes 7 and 8). To substantiate this finding further, we constructed reporters by replacing the main coding region of MRPL18 with *firefly* luciferase (Fluc). Consistent with the immunoblotting results of MRPL18 mutants, the chimeric C14A-Fluc exhibited the highest increase of Fluc expression in response to heat shock stress (**Fig. 2b**).

Having confirmed the stress-induced alternative translation of MRPL18 using mutants, we next sought to determine whether the wild type MRPL18 undergoes translational switch from the authentic AUG to the downstream CUG in response to heat shock stress. It is challenging to unequivocally monitor the newly synthesized MRPL18(cyto) within high basal levels of MRPL18(mito) pre-existed in cells before stress. To circumvent this limitation, we employed a reversible destabilization domain (DD) by fusing it to the COOH

terminus of MRPL18(WT) (Fig. 2c). This system permits temporal examination of newly synthesized MRPL18-DD after addition of Shield-1, a cell permeable drug<sup>20</sup>. HeLa cells transfected with plasmids expressing MRPL18-DD exhibited minimal anti-myc signals in the absence of Shield-1 (**Supplementary Fig. 2a**). Treatment with Shield-1 stabilized MRPL18-DD with a clear mitochondrial localization (**Fig. 2c** and **Supplementary Fig. 2b**). Remarkably, heat shock stress prior to Shield-1 addition resulted in substantial anti-myc signals in the cytosol as well as the nucleus (**Fig. 2c** and **Supplementary Fig. 2c**). This was not due to mitochondrion leakage, because the stress-induced Hsp60 remained exclusively in mitochondria after heat shock. This result confirms that heat shock stress triggers CUG-mediated alternative translation within the wild type sequence context of MRPL18.

### MRPL18(cyto) is dependent on eIF2 $\alpha$ phosphorylation

What is the mechanism underlying stress-induced alternative translation of MRPL18? We looked into eukaryotic initiation factor 2 $\alpha$  (eIF2 $\alpha$ ), whose phosphorylation regulates ATF4, a classical example of alternative translation triggered by many stress conditions<sup>21-24</sup>. Consistent with the previous report<sup>25</sup>, heat shock stress also triggered eIF2 $\alpha$  phosphorylation (**Supplementary Fig. 3a**). To address the role of eIF2 $\alpha$  phosphorylation in the alternative translation of MRPL18, we transfected MRPL18-Fluc reporters into a mouse embryonic fibroblast (MEF) cell line bearing a non-phosphorylatable eIF2 $\alpha$  in which the serine 51 (S/S) was mutated to an alanine (A/A)<sup>26</sup>. As expected, wild type MEF (S/S) cells showed the similar pattern of Fluc expression as HeLa cells (**Fig. 2d**). In particular, the CUG-only MRPL18 (C14A) exhibited the highest increase of Fluc (> 4 fold) in response to heat shock stress, whereas the expression level of the AUG-only MRPL18(G72A) remained unchanged. Remarkably, the stress responsiveness of MRPL18 (C14A) was completely abolished in MEF(A/A) cells (**Fig. 2d** and **Supplementary Fig. 3b**), indicating that the alternative translation of MRPL18 is dependent on eIF2 $\alpha$  phosphorylation.

### MRPL18(cyto) integrates into cytosolic 80S ribosomes

Considering the authentic role of MRPL18 is to constitute the ribosome complex within mitochondria, it is tempting to speculate that MRPL18(cyto) integrates into the cytosolic 80S ribosome complex under stress conditions. To test this hypothesis, we assessed the behavior of endogenous MRPL18 as well as transfected mutants in HeLa cells. We first purified cytosolic ribosome complexes using affinity immunoprecipitation (IP) in order to eliminate mitochondrial ribosome contamination. We also converted the polysome into monosome by RNase I digestion prior to IP to exclude indirect pull down of RNA binding proteins (**Fig. 3a**). Endogenous MRPL18, but not other mitochondrial proteins, was readily precipitated from stressed cells by either anti-RPL4 or anti-RPS6 antibodies (**Fig. 3a**, lane 2 and 6). In addition, endogenous MRPL18 was recovered from the polysome fraction after heat shock stress, and this re-distribution was sensitive to translation inhibitor CHX (**Supplementary Fig. 4**). Therefore, the cytosolic ribosome-associated MRPL18 is newly synthesized after stress. The incorporation of MRPL18(cyto) into the 80S ribosome complex was further corroborated by the similar feature of transfected MRPL18(ATG). Both co-sedimentation binding analysis and anti-myc IP revealed a robust association of MRPL18(ATG) with cytosolic ribosomes in a stress-dependent manner (**Fig. 3b**, lane 8 and

**3c**, lane 6). In contrast, the AUG-only MRPL18(G72A) did not co-precipitate with any cytosolic RPs before or after heat shock stress (**Fig. 3C**).

### Phosphorylated MRPL18(cyto) integrates into 80S ribosomes

Interestingly, very few transfected MRPL18(ATG) was associated with the 80S ribosome in unstressed cells in spite of comparable expression levels. To investigate the mechanism of stress-induced incorporation, we examined the phosphorylation status of MRPL18 using a Phos-tag acryl-amide gel. A MRPL18 band with slower migration was clearly discernable upon heat shock stress and sensitive to phosphatase treatment (**Fig. 4a**). Adding translation inhibitor CHX completely abolished this species, suggesting that phosphorylation occurs to the newly synthesized MRPL18 during stress. Importantly, the phosphorylated MRPL18 was exclusively found in the cytosolic fraction (**Fig. 4b**), and only the phosphorylated species was recovered from the cytosolic 80S ribosome (**Fig. 4c** and **4d**). We next searched for the kinase responsible for MRPL18 phosphorylation. Interestingly, MRPL18 was predicted to be a substrate of the tyrosine-protein kinase Lyn<sup>27</sup>. Indeed, both the Lyn-specific chemical inhibitor Bafetinib (**Fig. 5a**) and shRNA knockdown (**Fig. 5b**) reduced the phosphorylation level of MRPL18. Notably, Lyn is a member of the Src family, whose kinases activity is increased upon heat shock stress<sup>28</sup>. These results collectively indicate that both the production and function of MRPL18(cyto) is under tight control in response to stress.

### MRPL18(cyto) promotes stress protein synthesis during stress

The stress-inducible feature of MRPL18(cyto) is suggestive of its regulatory role in cytosolic stress response. To elucidate its physiological function, we knocked down MRPL18 in HeLa cells using small interference RNA (siRNA) SMARTpool. Reducing MRPL18 expression had minimal effects on cell growth and did not alter the rate of global protein synthesis (**Supplementary Fig. 5a**). In addition, we observed minimal effects of MRPL18 depletion on mitochondria translation after short term siRNA knockdown or long term lentivirus-based small hairpin RNA (shRNA) knockdown (**Supplementary Fig. 5b** and **5c**). However, upon heat shock treatment, the induction of Hsp70 expression in the cytosol was largely dampened in cells with MRPL18 knockdown when compared to cells transfected with control siRNA (**Fig. 6a**). To substantiate this finding further, we applied shRNA to HeLa cells and a mouse embryonic fibroblast (MEF) cell line (**Fig. 6b** and **Supplementary Fig. 6**). shRNA-mediated MRPL18 knockdown resulted in impaired Hsp70 induction in both cells after heat shock stress. This was not due to transcriptional deficiency of Hsp70 gene expression. In fact, MEFs with MRPL18 knockdown demonstrated even higher Hsp70 transcript levels than the control cells in response to heat shock stress (**Supplementary Fig. 6d**).

Given the *de novo* synthesis of MRPL18(cyto) relies on alternative translation, we reasoned that suppressing CUG initiation would have the similar effect as MRPL18 knockdown. Indeed, the stress-induced Hsp70 synthesis was substantially reduced in eIF2 $\alpha$  (A/A) cells whose eIF2 $\alpha$  is not phosphorylatable (**Fig. 6c**). Since the incorporation of MRPL18(cyto) into the 80S ribosome is phosphorylation-dependent, we examined the effects of reduced Lyn kinase activities in stress response. It is clear that treatment with either Lyn inhibitor

Bafetinib or Lyn knockdown dramatically suppressed the Hsp70 induction after heat shock stress (**Fig. 5a** and **5b**). The deficient Hsp70 synthesis is specific to MRPL18 because knocking down other mitochondrial ribosomal proteins did not influence the cytosolic stress response at all (**Supplementary Fig. 7a** and **7b**). These data collectively highlight MRPL18(cyto) as a critical mediator of cytosolic stress response.

### MRPL18(cyto) promotes ribosome engagement on stress mRNAs

The participation of MRPL18(cyto) in the Hsp70 synthesis suggests that a specialized ribosome might be required for mRNA translation under stress conditions. MRPL18 is a homolog of cytoplasmic RPL5 based on sequence alignment. Much like RPL5, MRPL18 also binds to 5S rRNA and is believed to import the 5S rRNA into mitochondria<sup>29</sup>. An *in vitro* RNA binding assay confirmed that 5S rRNA strongly associates with recombinant MRPL18(ATG) but not GFP (**Supplementary Fig. 7d** and **7e**). However, we found little evidence indicating that MRPL18 replaces RPL5 in binding to the 80S ribosome (**Fig. 3**). In fact, RPL5 knockdown also reduced Hsp70 synthesis after heat shock stress (**Supplementary Fig. 7c**). Notably, MRPL18 does not seem to interact with separated 40S or 60S subunits (**Supplementary Fig. 7f**). It is thus likely that MRPL18(cyto) serves as an extra RP in binding to the 80S ribosome. 5S rRNA forms the central protuberance of the large ribosomal subunit<sup>30</sup>. This region is of particular importance because it nears the place where the ribosomal large and small subunits, the decoded mRNA, as well as the peptidyl tRNA all come together. We postulate that the presence of an extra RP promotes 80S ribosome engagement on mRNAs under stress conditions. To test this hypothesis, we examined the distribution of Hsp70 mRNA in the polysome fractions of stressed MEF cells with or without MRPL18 knockdown (**Fig. 6d**). With comparable total mRNA levels, the Hsp70 transcript showed much less enrichment in the polysomes of MEF cells lacking MRPL18. In contrast,  $\beta$ -actin mRNA only exhibited minor reduction in the polysome of these cells presumably due to the delayed stress recovery as a result of impaired Hsp70 synthesis. Indeed, MEF cells lacking MRPL18 showed less polysome formation during stress recovery (**Fig. 6d**).

### MRPL18 is essential for induced thermotolerance

Because of the essential role of chaperone molecules in cell survival, we predict that cells lacking MRPL18 should have attenuated thermotolerance. Induced thermotolerance allows cells to survive a normally lethal temperature if they are first conditioned at a milder temperature. Without preconditioning, MEF cells with or without MRPL18 knockdown were equally susceptible to severe heat stress at 45°C for 1 h (**Fig. 7a**). Pre-exposure at 43°C for 30 min resulted in a nearly complete protection of control MEF cells from severe heat stress. However, the induced thermotolerance was no longer observed in MEFs with MRPL18 knockdown. As expected, the reduced cell viability in the absence of MRPL18 was largely due to increased apoptosis (**Fig. 7b**). In agreement with the suppressed chaperone biosynthesis in cells lacking MRPL18, re-introduction of Hsp70 by recombinant adenoviruses completely restored the thermotolerance (**Fig. 7c**). Given the broad range of chaperone function in cell physiology, it would be of much interest to investigate possible protective roles of MRPL18 against cellular stressors beyond heat shock.

## DISCUSSION

Cells in nearly all living organisms respond to heat shock stress by marked transcriptional alterations and rapid translational re-programming<sup>5</sup>. Despite severe inhibition of the translation machinery under stress conditions, efficient synthesis of stress proteins persists in a mechanism that was not completely understood. Here, we uncovered a molecular mechanism underlying the active translation of mRNAs highly expressed during stress. We show that heat shock stress triggers a previously unrecognized alternative translation of MRPL18, generating a cytoplasmic isoform of the mitochondrial ribosomal protein. Remarkably, the cytoplasmic version of MRPL18 incorporates into the 80S ribosome complex in a stress-dependent manner. The stress-induced formation of specialized ribosomes, together with the cap-independent translation initiation mechanism, ensures efficient translation of mRNAs under non-favorable conditions (**Fig. 7d**). Our results thus provide a new paradigm for translational regulation under stress conditions, which involves ribosome specialization after an initial alternative translation event.

A growing body of evidence suggests that ribosome heterogeneity prevails across species, under different developmental stages, and in varied tissues<sup>31,32</sup>. Variation in ribosome composition, in both rRNA and RPs, provides a regulatory mechanism to the translation machinery. A clear example is illustrated in *E. coli*, in which a stress-induced endonuclease MazF cleaves the 16S rRNA and removes the anti-Shine-Dalgarno sequence<sup>33</sup>. The resultant “stress ribosome” selectively translates the leaderless mRNAs, a group of transcripts also generated by MazF. In eukaryotes, certain RPs have been found to control transcript selectivity during translation. For example, RPL38 is required for translation of homeobox mRNAs<sup>34</sup>, whereas RPL40 appears to control translation of vesicular stomatitis virus mRNAs<sup>35</sup>. In this report, we discovered in mammalian cells an unusual mechanism that bestows the escape of HSP mRNA translation from the shutoff of global protein synthesis. Instead of altering the rRNA structure, the mammalian “stress ribosome” employs an extra RP that originally functions in mitochondria. MRPL18(cyto) incorporation may alter the ribosome conformation and/or stabilize the ribosome engagement on mRNAs that are highly expressed under stress conditions. Alternatively, the presence of MRPL18(cyto) may recruit additional factors facilitating initiation and elongation. In any means, stress-induced ribosome heterogeneity permits translational re-programming without re-building the entire translational machinery.

Another interesting phenomenon revealed by our data is the functional connection between mitochondrial and cytoplasmic ribosomes. The 55S mitochondrial ribosome differs substantially from the 80S ribosome in eukaryotic cytoplasm and the 70S ribosome in prokaryotes. In mammalian cells, the mitochondrial ribosome complex contains higher protein content than rRNA components<sup>14,36</sup>. Although many MRPs are distinctive and evolving rapidly, MRPL18 has a close homolog in *E. coli*. Unlike many other RPs, MRPL18 has apparently evolved to become a stress-inducible gene in mammals. The possession of an alternative translation feature further renders MRPL18 a critical regulator of stress response. We conclude that MRPL18 actively participates in stress adaptation by potentiating the cellular translation machinery to achieve a robust cytosolic stress response.

## ONLINE METHODS

### Cell lines and reagents

HeLa cells were maintained in Dulbecco's Modified Eagle's Medium (DMEM) with 10% fetal bovine serum (FBS). *HSF1*<sup>+/+</sup> and *HSF1*<sup>-/-</sup> MEFs were kindly provided by I. J. Benjamin (University of Utah). Cycloheximide (CHX), poly-U and puromycin were purchased from Sigma. MitoTracker, Mitochondria-GFP Alexa Fluor 488 or 546 labeled secondary antibodies [donkey anti-mouse IgG (H+L)] and Hoechst were purchased from Invitrogen. Anti-MRPL18 (HPA028774), anti-MRPL38 (HPA023054), anti-RPS20 (HPA003570), anti-RPL5 (HPA043717), anti-myc (C3956) and  $\beta$ -actin (A5441) monoclonal antibody was purchased from Sigma; anti-MRPS18B (16139-1-AP) and anti-RPL4 (11302-1-AP) was from Proteintech; anti-Hsp70 (SPA810) was from Enzo Life Sciences; anti-RPS6 (#2217), anti-HSP60 (#4870), anti-Caspase 3 (#9662) and cleaved Caspase 3 (#9661) antibody were from Cell Signaling. Dual luciferase kit was purchased from Promega. siRNA SMARTpools targeting human MRPL18 and control were purchased from Dharmacon. siRNA targeting human Lyn, MRPL38 and MRPS18B were purchase from Santa Cruz Biotechnology. Plasmids and siRNA transfections were performed using Lipofectamine 2000 (Invitrogen) following the manufacturer's instruction.

### Plasmids

MRPL18 cDNA was cloned from total RNAs extracted from HeLa cells by RT-PCR. The amplified MRPL18 cDNA contains both the 5'UTR and the coding sequence and was inserted into pcDNA3.1/myc-his (Invitrogen). For MRPL18 mutants, mutagenesis was performed using the QuikChange II site-directed mutagenesis kit following the manufacturer's instruction (Stratagene). For MRPL18-Fluc constructs, an *EcoR* I site downstream of the CTG codon was used to replace the MRPL18 with firefly luciferase (Fluc) derived from pGL3 (Promega). For MRPL18-DD constructs, the FKBP destabilized domain (DD) was amplified from pBMN and subcloned into pcDNA3.1/ MRPL18. All plasmids were confirmed by DNA sequencing.

### Lentiviral shRNAs

All shRNA targeting sequences were cloned into DECIPHER™ pRSI9-U6-(sh)-UbiC-TagRFP-2A-Puro (CELLECTA). shRNA targeting sequences were based on RNAi consortium at Broad Institute (<http://www.broad.mit.edu/rnai/trc>). MRPL18(human): 5' CTCAGAGAATCTATGAATAAA 3'; MRPL18(mouse): 5' CCAAAGGAAAGCATC TGCATT 3'; control sequence: 5' AACAGTCGCGTTTGCGACTGG 3'. Lentiviral particles were packaged using Lenti-X 293T cells (Clontech). Virus-containing supernatants were collected at 48-h after transfection and filtered to eliminate cells, and target cells were infected in the presence of 8  $\mu\text{g ml}^{-1}$  polybrene. 24-h later, cells were selected with 5  $\mu\text{g ml}^{-1}$  puromycin.

### Immunoprecipitation

Cells were washed twice with PBS and lysed in ice-cold lysis buffer [20 mM HEPES (pH 7.4), 150 mM NaCl, 5 mM MgCl<sub>2</sub>, 0.5 mM DTT, 1X EDTA-free complete protease



inhibitor (Roche), 100  $\mu\text{g ml}^{-1}$  CHX, 20  $\mu\text{g ml}^{-1}$  Poly-U] supplemented with 1% NP-40. Cell lysates were incubated on ice for 1-h and then treated with 2  $\mu\text{l}$  RNase I (Ambion) for another 1-h at 4°C. Lysates were spun at 20,000  $\times$  g for 10 min at 4°C and supernatants were collected followed by incubation with anti-myc agarose beads (Sigma) at 4 °C for overnight. Immunoprecipitates were washed 4 times with gradient buffer [10 mM HEPES (pH 7.4), 150 mM NaCl, 5 mM MgCl<sub>2</sub>] containing 1% NP-40. The washed beads were resuspended in 1x SDS sample buffer [100 mM Tris (pH 6.8), 2% SDS, 15% glycerol, 5%  $\beta$ -mercaptoethanol, 0.1% bromophenol blue), boiled for 10 min, and analyzed by immunoblotting.

### Immunoblotting

Cells were lysed on ice in TBS buffer [50 mM Tris (pH7.5), 150 mM NaCl, 1 mM EDTA] containing protease inhibitor cocktail tablet, 1% Triton X-100, and 2 U ml<sup>-1</sup> DNase. After incubating on ice for 30 min, the lysates were heated for 10 min in SDS/PAGE sample buffer [50 mM Tris (pH6.8), 100 mM dithiothreitol, 2% SDS, 0.1% bromophenol blue, 10% glycerol). Proteins were resolved on SDS-PAGE and transferred to Immobilon-P membranes (Millipore). For Phos-tag SDS-PAGE, 50  $\mu\text{M}$  Phos-tag Acrylamide (WAKO) and 50  $\mu\text{M}$  MnCl<sub>2</sub> (Sigma) were added to 12% acrylamide gel, and performed electrophoresis in a manner identical to standard SDS-PAGE. After electrophoresis, Mn<sup>2+</sup> was removed from phos-tag gel by incubation with 1x Transfer buffer containing 1 mM EDTA for 10 min. EDTA was then removed by incubation with 1x Transfer buffer for another 10 min before the transfer. Membranes were blocked for 1-h in TBS containing 5% BSA, followed by incubation with primary antibodies. After incubation with horseradish peroxidase-coupled secondary antibodies, immunoblots were developed using enhanced chemiluminescence (ECL<sup>Plus</sup>, GE Healthcare).

### In vitro RNA synthesis and binding assay

Full-length human 5S and 5.8S rRNA were amplified by using a forward primer carrying a T7 polymerase target sequence (underlined) and a reverse primer:

5S rRNA forward: 5'- TAATACGACTCACTATAGGGGTCTACGGCCATACCACC CTG -3'; 5S rRNA reverse: 5'- AAAGCCTACAGCACCCGGTAT -3'; 5.8S rRNA forward: 5'- TAATACGACTCACTATAGGG GACTCTTAGCGGTGGATC -3'; 5.8S rRNA reverse: 5'- AAGCGACGCTCAGACAGGC -3'.

Purified PCR product was used as template for in vitro transcription. In vitro transcription was carried out using MEGAshortscript kit (Ambion) according to the manufacturer's instruction. The coding sequence of MRPL18 without mitochondrial target sequence (MRPL18 (ATG)) was subcloned into pET-30a vector. *E. coli* strain BL21(DE3) was used as the host for protein expression and proteins were purified by Ni-NTA agarose (Qiagen). Binding of MRPL18 (ATG) to 5 S rRNAs was measured by a shift in the mobility of the RNA in 1.8% Agarose gels run at room temperature at 100 V. Binding reactions were performed in buffer containing 20 mM HEPES, pH 8.0; 30 mM NH<sub>4</sub>Cl; 100 mM KCl; 0.5 mM MgCl<sub>2</sub>; 1 mM DTT; 4% glycerol; 0.1% Nonidet P-40; acetylated bovine serum albumin (0.05 mg/ml); ribonuclease inhibitor (0.2 unit/ml of RNase OUT). Protein and RNA at the

indicated concentrations were mixed gently and incubated at room temperature for 30min. After addition of Hi-Density TBE Sample Buffer (Invitrogen), the reactions were loaded onto a 1.8% Agarose gel and electrophoresed in TAE buffer (40mM Tris acetate, 1mM EDTA) at 100 V for 30min. Following electrophoresis, the RNA was visualized by ethidium bromide staining.

### Polysome profiling analysis

Polysome buffer [10 mM HEPES (pH 7.4), 100 mM KCl, 5 mM MgCl<sub>2</sub>, 100 µg ml<sup>-1</sup> cycloheximide and 2% Triton X-100] was used to prepare sucrose solutions. Sucrose density gradients (15%- 45% w/v) were freshly made in SW41 ultracentrifuge tubes (Beckman) using a Gradient Master (BioComp Instruments) according to manufacturer's instructions. Cells were pre-treated with 100 µg ml<sup>-1</sup> cycloheximide for 3 min at 37°C to stabilize ribosomes on mRNAs followed by washing using ice-cold PBS containing 100 µg ml<sup>-1</sup> cycloheximide. Cells were then lysed by scraping extensively in polysome lysis buffer. Cell debris were removed by centrifugation at 14,000 rpm for 10 min at 4°C. 600 µl of supernatant was loaded onto sucrose gradients followed by centrifugation for 100 min at 38,000 rpm 4°C in a SW41 rotor. Separated samples were fractionated at 0.750 ml/min through an automated fractionation system (ISCO) that continually monitors OD<sub>254</sub> values. Fractions were collected with 0.5 min interval. An aliquot of ribosome fraction was used to extract total RNA using Trizol LS reagent (Invitrogen) for real-time PCR analysis or were heated at 98 °C for 10 min in SDS sample buffer [50 mM Tris-HCl (pH6.8), 100 mM dithiothreitol, 2% SDS, 0.1% bromophenol blue, 10% glycerol] for western blot analysis.

For polysome concentration, fractions corresponding to more than 2 ribosomes were pooled and diluted 1:1 with gradient buffer. Polysomes were pelleted by centrifugation for 2 hours 4°C at 300,000 × g in polycarbonate centrifuge tubes (Beckman 349622) in a TLA110 rotor (Beckman) using a tabletop ultracentrifuge (Optima MAX, Beckman). Polysome pellet was re-suspended in 1x SDS sample buffer for western blot analysis.

### Ribosome sucrose cushion

Ribosome sucrose cushion were conducted using a previously described protocol with minor modifications<sup>37</sup>. In brief, Hela cells were collected in lysis buffer [20 mM Tris (pH 7.4), 10 mM MgCl<sub>2</sub>, 300 mM KCl, 10 mM dithiothreitol, 100 units/ml RNase OUT, 20 µg ml<sup>-1</sup> Poly-U and 100 µg ml<sup>-1</sup> cycloheximide]. Cell lysates were incubated on ice for 1-h and then centrifuged at 12,500 × g for 10 min to remove mitochondria and debris. The supernatant was layered over 1 ml of 1M sucrose cushion followed by centrifugation at 60,000 rpm for 2-h in a Beckman TLA-110 rotor. The ribosome-containing pellet was rinsed twice with 200 µl ice cold water and re-suspended in 1x SDS sample buffer for western blot analysis.

### RNA isolation and PCR

Total cellular RNA was extracted using the TRIzol reagent (Invitrogen) according to the manufacturer's instruction. Contaminating DNA was digested by pre-treatment with RNase-free DNase (Ambion). Single strand cDNA synthesis was carried out using the high-capacity cDNA reverse transcription kit (Applied Biosystems) followed by standard PCR reactions. Real-time PCR reactions were performed using Power SYBR Green Master Mix (Applied

Biosystems) using a LightCycler® 480 *Real-time PCR System (Roche)*. Gene expression was normalized to  $\beta$ -actin cDNA levels and calculated as a relative gene expression using  $2^{-Ct}$  method.

Oligonucleotide primers are as follows: Human MRPL18: forward 5'-CATCAG AATGGCAAGGTTGTG-3' and reverse 5'-AAGTTGATTCCCGCCTCTAAG-3'; Mouse MRPL18: forward 5'-AGCAAAGGAAGATAGGGCAC-3' and reverse 5'-ACA GACATTTCCAGAACCGC-3'; Human HSPA1A: forward 5'-TGTGTAACCCCATCA TCAGC-3' and reverse 5'-TCTTGGAAGGCCCTAATC-3'; Mouse HSPA1A: forward 5'-TGGTGCAGTCCGACATGAAG-3' and reverse 5'-GCTGAGAGTCGTTG AAGTAGGC-3'; Human  $\beta$ -actin: forward 5'-AGCCTCGCCTTTGCCGA-3' and reverse 5'-GCGCGGCGATATCATCATC-3'; Mouse  $\beta$ -actin: forward 5'-TTGCTGACAGGA TGCAGAAG-3' and reverse 5'-ACTCCTGCTTGCTGATCCACAT-3'. Quantitation of target genes of each fraction was normalized using the reference Firefly luciferase. Primers used are forward 5'-ATCCGGAAGCGACCAACGCC-3' and reverse 5'-GTCC GGAAGACCTGCCACGC-3'.

### [<sup>35</sup>S] metabolic labeling

Cells were washed with DPBS (pH 7.0, Invitrogen) prior to incubation in methionine-free DMEM (Invitrogen) for 15 min at 37°C. After quick centrifugation, cells were re-suspended in labeling media [methionine-free DMEM supplemented with 10% FBS and 10  $\mu$ Ci ml<sup>-1</sup> [<sup>35</sup>S] mix (Perkin Elmer)]. At the indicated time points, aliquots were transferred to ice-cold stop buffer (DMEM supplemented with 1 mg ml<sup>-1</sup> L-methionine, 1 mg ml<sup>-1</sup> L-cystine and 100  $\mu$ g ml<sup>-1</sup> cycloheximide). Cells were centrifuged at 12,500 rpm for 5 min and the cell pellets were washed with ice-cold DPBS supplemented with 1 mg ml<sup>-1</sup> of L-methionine and L-cystine with 100  $\mu$ g ml<sup>-1</sup> cycloheximide. The washed cell pellets were lysed in ice-cold lysis buffer [10 mM HEPES (pH 7.4), 100 mM KCl, 5 mM MgCl<sub>2</sub>, 100  $\mu$ g ml<sup>-1</sup> cycloheximide and 2% Triton X-100] for 30 min followed by centrifugation at 12,500 rpm 4°C for 10 min. The supernatant was collected and precipitated with 10% Trichloroacetic acid (Sigma). The mixture was heated for 10 min at 90°C followed by 10 min incubation on ice. The precipitates were collected on GF/C filter membranes (Whatman) followed by washing with 10% TCA and 100% ethanol, respectively. The dried membrane was measured for [<sup>35</sup>S] incorporation using scintillation counting (Beckman Coulter).

For mitochondria translation, cells were pretreated with 100  $\mu$ g ml<sup>-1</sup> cycloheximide for 5 min prior to a 1-h metabolic labeling in labeling media supplemented with 100  $\mu$ g ml<sup>-1</sup> cycloheximide in the absence or presence of 100  $\mu$ g ml<sup>-1</sup> chloramphenicol. Whole cell lysates were separated on a 12% SDS-PAGE gel followed by autoradiography.

### Luciferase assay

Real time measurements of Fluc activity were recorded at 37°C with 5% CO<sub>2</sub> using KronosDio Luminometer (Atto) as previously described<sup>11</sup>. In brief, cells were plated on 35-mm dishes and transfected with plasmids encoding Fluc. 12 hours after transfection, cells were subjected to heat shock (43°C, 1-h), 1 mM luciferase substrate D-luciferin (Regis Tech) was added into the culture medium. For Hsp70-Fluc experiments, cells were subjected

to heat shock 1-h after transfection, followed by the addition of 1 mM luciferase substrate D-luciferin.

### Immunofluorescence staining

Cells grown on glass coverslips were fixed in 4% paraformaldehyde and permeabilized by 0.2% Triton X-100. After blocking in 2% BSA in PBS, fixed cells were incubated with the primary antibody at 4°C overnight followed by 1-h incubation at room temperature with Alexa Fluor-labeled secondary antibodies. Cells were then washed with PBS and incubated for 5 min in PBS supplemented with Hoechst to counter-stain the nuclei. After final wash with PBS, cover slips were mounted onto slides and viewed using a confocal microscope (Zeiss LSM710).

### Cell viability assay

MEF cells infected with lentiviruses expressing shRNA targeting MRPL18 or Scramble control were selected for stable cell lines. To induce heat shock response, cells were incubated at 43°C water bath for 30 minutes and allowed to recover at 37 °C for 5 hours (Pre-HS). Lethal heat stress (45 °C for 1 hour) was subsequently applied followed by incubation at 37 °C for 24 hours. Cells were then used for viability assay using Cell Counting Kit-8 (Dojindo Molecular Technologies) or collected for Western Blot analysis. For rescue assay, 24 hours before lethal heat stress, cells were infected with recombinant adenoviruses encoding GFP or Hsp70 at ~ 10 MOI followed by viability assay.

### Supplementary Material

Refer to Web version on PubMed Central for supplementary material.

### ACKNOWLEDGEMENTS

We'd like to thank J.W. Yewdell and T. Fox for critical reading of the manuscript. We also thank I. Benjamin (University of Utah) for providing *HSF1*<sup>+/+</sup> and *HSF1*<sup>-/-</sup> MEFs, R. Kaufman (The Sanford Burnham Medical Research Institute) for eIF2α(S/S) and eIF2α(A/A) MEFs, and T. Wandless (Stanford) for plasmids encoding FKBP destabilizing domain. This work was supported in part by US National Institutes of Health training grants to R.A.C. and C.S.C. B.L. was a recipient of the Genomics Scholar's Award from Center for Vertebrate Genomics at Cornell. This work was primarily supported by grants to S.-B.Q. from US National Institutes of Health (DP2 OD006449, R01AG042400), Ellison Medical Foundation (AG-NS-0605-09), and US Department of Defense (W81XWH-14-1-0068).

### REFERENCES

1. Holcik M, Sonenberg N. Translational control in stress and apoptosis. *Nat Rev Mol Cell Biol.* 2005; 6:318–327. [PubMed: 15803138]
2. Spriggs KA, Bushell M, Willis AE. Translational regulation of gene expression during conditions of cell stress. *Mol Cell.* 2010; 40:228–237. [PubMed: 20965418]
3. Jackson RJ, Hellen CU, Pestova TV. The mechanism of eukaryotic translation initiation and principles of its regulation. *Nat Rev Mol Cell Biol.* 2010; 11:113–127. [PubMed: 20094052]
4. Panniers R. Translational control during heat shock. *Biochimie.* 1994; 76:737–747. [PubMed: 7893824]
5. Richter K, Haslbeck M, Buchner J. The heat shock response: life on the verge of death. *Mol Cell.* 2010; 40:253–266. [PubMed: 20965420]

6. Morimoto RI. Regulation of the heat shock transcriptional response: cross talk between a family of heat shock factors, molecular chaperones, and negative regulators. *Genes Dev.* 1998; 12:3788–3796. [PubMed: 9869631]
7. Anckar J, Sistonen L. Regulation of HSF1 function in the heat stress response: implications in aging and disease. *Annu Rev Biochem.* 2011; 80:1089–1115. [PubMed: 21417720]
8. McGarry TJ, Lindquist S. The preferential translation of *Drosophila* hsp70 mRNA requires sequences in the untranslated leader. *Cell.* 1985; 42:903–911. [PubMed: 4053186]
9. Klemenz R, Hultmark D, Gehring WJ. Selective translation of heat shock mRNA in *Drosophila melanogaster* depends on sequence information in the leader. *EMBO J.* 1985; 4:2053–2060. [PubMed: 2933251]
10. Rubtsova MP, et al. Distinctive properties of the 5'-untranslated region of human hsp70 mRNA. *J Biol Chem.* 2003; 278:22350–22356. [PubMed: 12682055]
11. Sun J, Conn CS, Han Y, Yeung V, Qian SB. PI3K-mTORC1 attenuates stress response by inhibiting cap-independent Hsp70 translation. *J Biol Chem.* 2011; 286:6791–6800. [PubMed: 21177857]
12. Moore PB. How should we think about the ribosome? *Annu Rev Biophys.* 2012; 41:1–19. [PubMed: 22577819]
13. Kressler D, Hurt E, Bassler J. Driving ribosome assembly. *Biochim Biophys Acta.* 2010; 1803:673–683. [PubMed: 19879902]
14. Christian BE, Spremulli LL. Mechanism of protein biosynthesis in mammalian mitochondria. *Biochim Biophys Acta.* 2012; 1819:1035–1054. [PubMed: 22172991]
15. Lee S, Liu B, Huang SX, Shen B, Qian SB. Global mapping of translation initiation sites in mammalian cells at single-nucleotide resolution. *Proc Natl Acad Sci U S A.* 2012; 109:E2424–2432. [PubMed: 22927429]
16. Trinklein ND, Murray JI, Hartman SJ, Botstein D, Myers RM. The role of heat shock transcription factor 1 in the genome-wide regulation of the mammalian heat shock response. *Mol Biol Cell.* 2004; 15:1254–1261. [PubMed: 14668476]
17. Mendillo ML, et al. HSF1 drives a transcriptional program distinct from heat shock to support highly malignant human cancers. *Cell.* 2012; 150:549–562. [PubMed: 22863008]
18. Qian SB, McDonough H, Boellmann F, Cyr DM, Patterson C. CHIP-mediated stress recovery by sequential ubiquitination of substrates and Hsp70. *Nature.* 2006; 440:551–555. [PubMed: 16554822]
19. Margeot A, et al. In *Saccharomyces cerevisiae*, ATP2 mRNA sorting to the vicinity of mitochondria is essential for respiratory function. *EMBO J.* 2002; 21:6893–6904. [PubMed: 12486010]
20. Banaszynski LA, Chen LC, Maynard-Smith LA, Ooi AG, Wandless TJ. A rapid, reversible, and tunable method to regulate protein function in living cells using synthetic small molecules. *Cell.* 2006; 126:995–1004. [PubMed: 16959577]
21. Sonenberg N, Hinnebusch AG. New modes of translational control in development, behavior, and disease. *Mol Cell.* 2007; 28:721–729. [PubMed: 18082597]
22. Harding HP, Calton M, Urano F, Novoa I, Ron D. Transcriptional and translational control in the Mammalian unfolded protein response. *Annu Rev Cell Dev Biol.* 2002; 18:575–599. [PubMed: 12142265]
23. Vattem KM, Wek RC. Reinitiation involving upstream ORFs regulates ATF4 mRNA translation in mammalian cells. *Proc Natl Acad Sci U S A.* 2004; 101:11269–11274. [PubMed: 15277680]
24. Wek RC, Jiang HY, Anthony TG. Coping with stress: eIF2 kinases and translational control. *Biochem Soc Trans.* 2006; 34:7–11. [PubMed: 16246168]
25. Duncan RF, Hershey JW. Protein synthesis and protein phosphorylation during heat stress, recovery, and adaptation. *J Cell Biol.* 1989; 109:1467–1481. [PubMed: 2793930]
26. Scheuner D, et al. Translational control is required for the unfolded protein response and in vivo glucose homeostasis. *Mol Cell.* 2001; 7:1165–1176. [PubMed: 11430820]
27. Yamanashi Y, et al. The yes-related cellular gene lyn encodes a possible tyrosine kinase similar to p56lck. *Mol Cell Biol.* 1987; 7:237–243. [PubMed: 3561390]

28. Lin RZ, Hu ZW, Chin JH, Hoffman BB. Heat shock activates c-Src tyrosine kinases and phosphatidylinositol 3-kinase in NIH3T3 fibroblasts. *J Biol Chem.* 1997; 272:31196–31202. [PubMed: 9388274]
29. Smirnov A, Entelis N, Martin RP, Tarassov I. Biological significance of 5S rRNA import into human mitochondria: role of ribosomal protein MRP-L18. *Genes Dev.* 2011; 25:1289–1305. [PubMed: 21685364]
30. Szymanski M, Barciszewska MZ, Erdmann VA, Barciszewski J. 5 S rRNA: structure and interactions. *Biochem J.* 2003; 371:641–651. [PubMed: 12564956]
31. Xue S, Barna M. Specialized ribosomes: a new frontier in gene regulation and organismal biology. *Nat Rev Mol Cell Biol.* 2012; 13:355–369. [PubMed: 22617470]
32. Gilbert WV. Functional specialization of ribosomes? *Trends Biochem Sci.* 2011; 36:127–132. [PubMed: 21242088]
33. Vesper O, et al. Selective translation of leaderless mRNAs by specialized ribosomes generated by MazF in *Escherichia coli*. *Cell.* 2011; 147:147–157. [PubMed: 21944167]
34. Kondrashov N, et al. Ribosome-mediated specificity in Hox mRNA translation and vertebrate tissue patterning. *Cell.* 2011; 145:383–397. [PubMed: 21529712]
35. Lee AS, Burdeinick-Kerr R, Whelan SP. A ribosome-specialized translation initiation pathway is required for cap-dependent translation of vesicular stomatitis virus mRNAs. *Proc Natl Acad Sci U S A.* 2013; 110:324–329. [PubMed: 23169626]
36. O'Brien TW. Properties of human mitochondrial ribosomes. *IUBMB Life.* 2003; 55:505–513. [PubMed: 14658756]
37. Mazumder B, et al. Regulated release of L13a from the 60S ribosomal subunit as a mechanism of transcript-specific translational control. *Cell.* 2003; 115:187–198. [PubMed: 14567916]

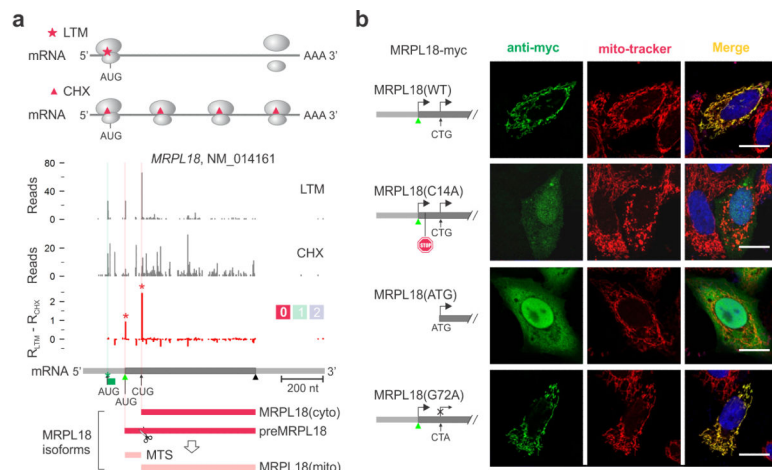


**Figure 1. MRPL18 undergoes alternative translation to produce a cytosolic isoform**

**(a)** Schematic of GTI-seq using translation inhibitors lactimidomycin (LTM) and cycloheximide (CHX) (top panel). Raw reads count per nt position of *MRPL18* are plotted as bar graph. The processed LTM reads density is color-coded by the corresponding reading frame and the identified TIS positions are marked by asterisk. The bottom panel shows the predicted isoforms of MRPL18.

**(b)** Immunostaining of HeLa cells transfected with MRPL18 wild type and mutants listed in the left panel. Anti-myc is shown in green channel and mito-tracker shown in red channel. DAPI was used for nuclear counterstaining. Bar, 10  $\mu$ m.

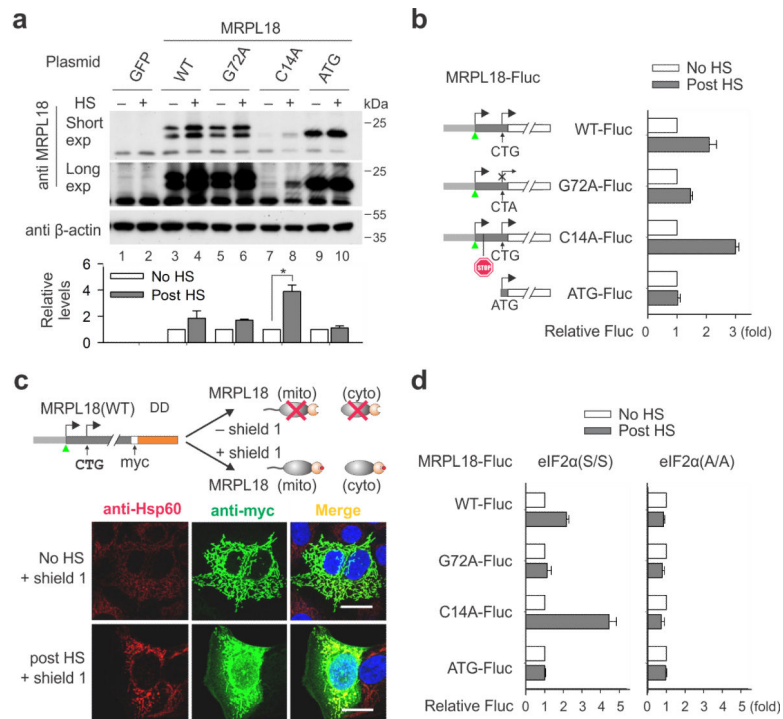


### Figure 2. MRPL18 Undergoes Alternative Translation in a Stress-Dependent Manner

**(a)** Representative immunoblot results of HeLa cells transfected with plasmids as indicated before heat shock or 2.5 h after heat shock (43°C, 1 h). Top bands are un-cleaved MRPL18 precursors. β-actin is used as loading control. The bottom panel shows the relative levels of transgenes (small isoform) normalized to β-actin. Error bars, s.e.m. ( $n = 3$  cell cultures,  $* p < 0.01$  by two-tailed Student's test).

**(b)** Fluc reporter assays in HeLa cells transfected with MRPL18-Fluc constructs listed in the left panel. Fluc activities after heat shock were normalized with non-stressed cells. Error bars, s.e.m. ( $n = 3$  cell cultures).

**(c)** Immunostaining of HeLa cells transfected with MRPL18-DD with or without heat shock in the presence of shield-1. The top panel shows schematic of MRPL18-DD fusion protein in the absence or presence of shield 1. Anti-Hsp60 antibody is shown in red channel and anti-myc shown in green channel and. Bar, 10 μm.

**(d)** Fluc reporter assays in eIF2α(S/S) and eIF2α(A/A) MEF cells transfected with MRPL18-Fluc constructs shown in (b). Fluc activities after heat shock were normalized with non-stressed cells. Error bars, s.e.m. ( $n = 3$  cell cultures).



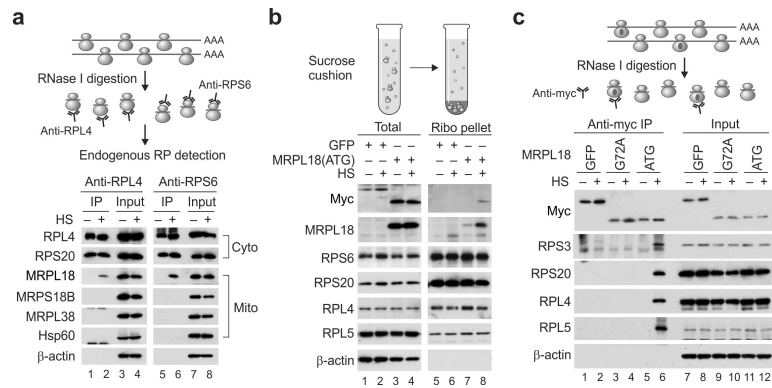


**Figure 3. Cytosolic MRPL18 incorporates into the 80S ribosome in a stress-dependent manner**

**(a)** Detection of MRPL18 from endogenous ribosomes purified from HeLa cells with or without heat shock. After RNase I digestion, cell lysates were immunoprecipitated using anti-RPL4 (left panel) or anti-RPS6 (right panel) antibody. Both the input and the immunoprecipitates were immunoblotted using antibodies as indicated.

**(b)** Detection of myc-tagged MRPL18(ATG) from endogenous ribosomes isolated from HeLa cells with or without heat shock. HeLa cells transfected with GFP were used as control. Sucrose cushion was used to isolate ribosomes. Both the total and the ribosome pellet were immunoblotted using antibodies as indicated.

**(c)** Detection of cytosolic ribosomal proteins from anti-myc immunoprecipitates in HeLa cells transfected with myc-tagged MRPL18(ATG) with or without heat shock. HeLa cells transfected with GFP and MRPL18(G72A) were used as controls. Cell lysates were treated with RNase I prior to anti-myc IP. Both the input and the immunoprecipitates were immunoblotted using antibodies as indicated.

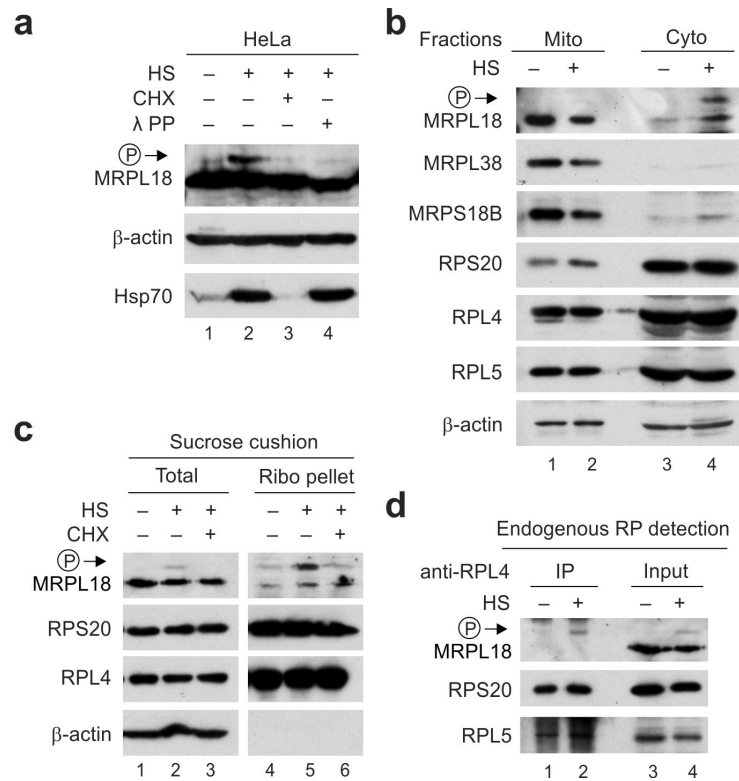


**Figure 4. Cytosolic MRPL18 incorporates into the 80S ribosome in a phosphorylation-dependent manner**

**(a)** Detection of phosphorylated MRPL18 in HeLa cells with or without heat shock stress. Whole cell lysates with or without λ phosphatase treatment were subject to Phos-tag acryl-amide gel (MRPL18 only) or standard PAGE followed by immunoblotting. CHX treatment during heat shock was included to demonstrate phosphorylation of newly synthesized MRPL18.

**(b)** Detection of phosphorylated MRPL18 in HeLa cell fractions with or without heat shock stress. Whole cell lysates of HeLa cells with or without heat shock were separated using mitochondria fractionation kit. Immunoblotting was conducted after separation on a Phos-tag acryl-amide gel (MRPL18 only) or standard PAGE.

**(c)** Detection of phosphorylated MRPL18 in ribosome fractions of HeLa cell with or without heat shock stress. Ribosome fractions were prepared by sucrose cushion. Both the total and the ribosome pellet were subjected to Phos-tag acryl-amide gel (MRPL18 only) or standard PAGE followed by immunoblotting.

**(d)** Detection of phosphorylated MRPL18 in ribosomes purified from HeLa cell with or without heat shock stress. After RNase I digestion, cell lysates were immunoprecipitated using anti-RPL4 antibody. Both the input and the immunoprecipitates were subject to Phos-tag acryl-amide gel (MRPL18 only) or standard PAGE followed by immunoblotting.

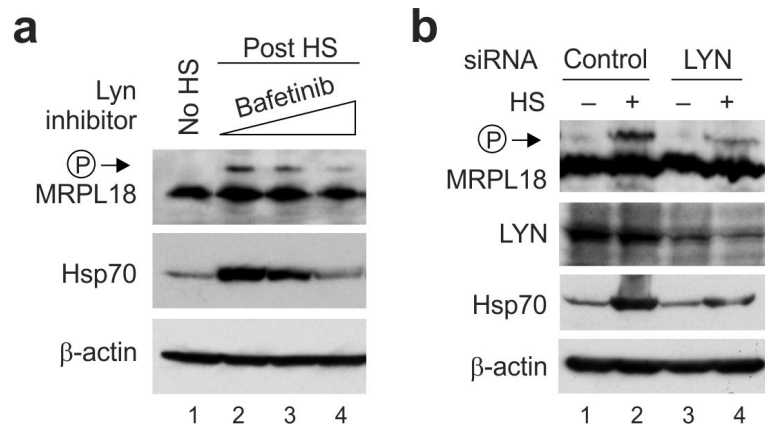


**Figure 5. Cytosolic MRPL18 undergoes Lyn-mediated phosphorylation**

**(a)** Detection of phosphorylated MRPL18 in HeLa cells in the presence of increasing doses of Bafetinib immediately after heat shock stress. Whole cell lysates were subject to Phos-tag acryl-amide gel (MRPL18 only) or standard PAGE followed by immunoblotting.

**(b)** Detection of phosphorylated MRPL18 in HeLa cells transfected with siRNA SMARTpool targeting Lyn or scramble control. Whole cell lysates were subject to Phos-tag acryl-amide gel (MRPL18 only) or standard PAGE followed by immunoblotting.

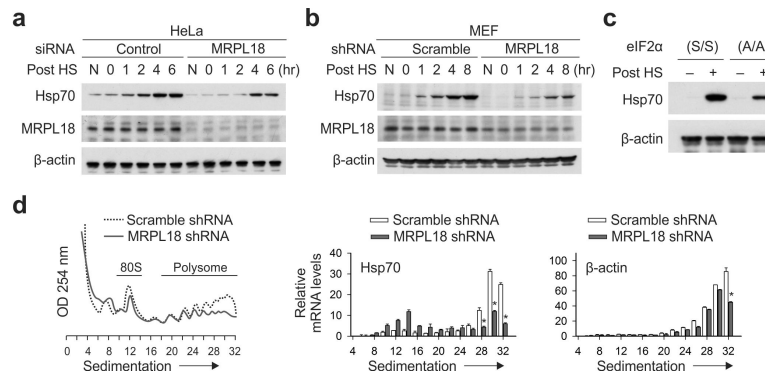


**Figure 6. Cytosolic MRPL18 promotes Hsp70 biosynthesis after heat shock stress**

**(a)** Examination of heat shock-induced Hsp70 synthesis in HeLa cells transfected with siRNA SMARTpool targeting MRPL18 or scramble control. Cells were collected at indicated times after heat shock followed by immunoblotting. N: no heat shock.

**(b)** Examination of heat shock-induced Hsp70 synthesis in MEF cells infected with lentiviruses expressing shRNA targeting MRPL18 or scramble control. Cells were subject to heat shock treatment and collected at indicated times after heat shock followed by immunoblotting. N: no heat shock.

**(c)** Examination of heat shock-induced Hsp70 synthesis in eIF2 $\alpha$ (S/S) and eIF2 $\alpha$ (A/A) MEF cells after heat shock stress.

**(d)** Examination of polysome-enriched Hsp70 mRNA in MEF cells infected with shRNA lentiviruses expressing shRNA targeting MRPL18 or scramble control. Polysome fractions were used to extract total RNA followed by qPCR measuring Hsp70 and  $\beta$ -actin mRNA levels. Relative levels are normalized to the total. Error bars, s.e.m. ( $n = 3$  cell cultures, \*  $p < 0.05$  by two-tailed Student's test).

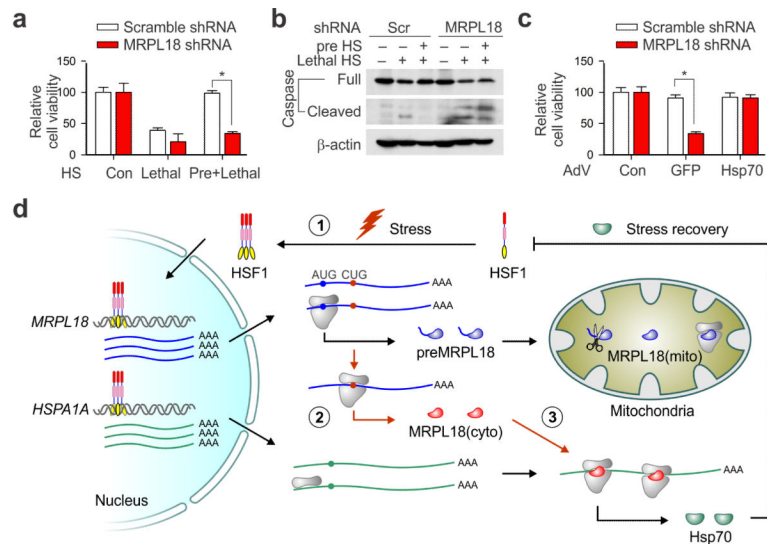


**Figure 7. Cytosolic MRPL18 is essential for induced thermal tolerance**

**(a)** Thermal tolerance analysis of MEF cells lacking MRPL18. MEF cells infected with shRNA targeting MRPL18 or scramble control were primed with mild heat shock (43°C for 30 min) followed by 37°C recovery for 5 h. Subsequent severe heat shock (45°C for 1 h) was then applied followed by cell viability assay. Error bars, s.e.m. ( $n = 4$  cell cultures, \*  $p < 0.01$  by two-tailed Student's test).

**(b)** Examination of apoptotic markers in MEF cells as (A) by immunoblotting using antibodies as indicated.

**(c)** Thermal tolerance assays of MEF cells after re-introduction of Hsp70. MEF cells as (A) were infected with recombinant adenoviruses encoding GFP or Hsp70 followed by thermal tolerance analysis. Error bars, s.e.m. ( $n = 3$  cell cultures, \*  $p < 0.01$  by two-tailed Student's test).

**(d)** A model for MRPL18 in translational control during stress conditions. Stress conditions like heat shock trigger trimerization and activation of HSF1 (step 1), which turns on genes including *MRPL18* and *HSPA1A*. In non-stressed cells, MRPL18 translation is initiated from the annotated AUG, generating MRPL18 containing mitochondria localization signal (blue). In stressed cells, MRPL18 undergoes alternative translation by using the downstream CUG start codon, producing a cytoplasmic isoform of MRPL18 (red) (step 2). MRPL18(cyto) incorporates into the 80S ribosome complex, facilitating the engagement of mRNAs highly expressed under stress, such as *HSPA1A* (green) (step 3). The efficient synthesis of heat shock proteins contributes to stress recovery.